Introduction to Turbulent Flow

Turbulent Flow. In turbulent flow, the velocity components and other variables (e.g. pressure, density - if the fluid is compressible, temperature - if the temperature is not uniform) at a point fluctuate with time in an apparently random fashion. In general, turbulent flow is time-dependent, rotational, and three dimensional – thus, methods such as developed for potential flow in handout 13 do not work. For instance, measurement of the velocity component v_1 at some stationary point in the flow may produce a plot as shown in Figure 1. In Figure 1, the velocity can be regarded as consisting of an average value $\overline{v_1}$ indicated by the dashed line, plus a random fluctuation v_1'

$$v_1(t) = \overline{v_1}(t) + v_1'(t) \tag{1}$$

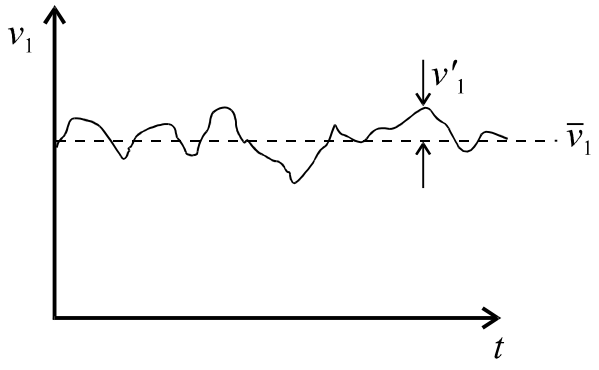

Figure 1

Similarly, other variables may also fluctuate, for example

$$p(t) = \overline{p}(t) + p'(t) \tag{2}$$

$$\rho(t) = \overline{\rho}(t) + \rho'(t) \tag{3}$$

The overscore denotes average values and the prime denotes fluctuations. Turbulence will always occur for sufficiently high *Re* numbers, regardless of the geometry of flow under consideration. The origin of turbulence rests in small perturbations imposed on the flow; for instance, by wall roughness, by small variations in fluid density, by mechanical vibrations, etc. At low *Re* numbers such disturbances are damped out by the fluid viscosity and the flow remains laminar, but at high *Re* (when convective momentum transport dominates over viscous forces) they can grow and propagate, giving rise to the chaotic phenomena perceived as turbulence. Turbulent flows can be very difficult to analyze. In this handout, some of the simplest concepts pertinent to turbulent flows are introduced.

Statistical Averaging of the Differential Equations of Fluid Mechanics. The differential equations of mass, momentum and energy balance express fundamental physical laws and therefore hold for turbulent flow just as they do for laminar flow. If all the perturbations acting on the flow can be also mathematically modeled, then these equations could be solved for the flow properties (velocity, pressure, etc.) of interest. However, this is generally too difficult a problem. An easier task is to solve "**time-averaged**" versions of these equations in which some of the fluctuation contributions are averaged out. As we shall see the solution to such equations provides less detailed, but still very useful, information.

Before considering how the differential equations should be time-averaged, it is helpful to establish several rules. First of all, we define a time-averaged quantity $\bar{a}(t)$ as the average of the instantaneous quantity $a = \bar{a} + a'$ over a time period T,

$$\bar{a}(t) \equiv \frac{1}{T}\int_{t-0.5T}^{t+0.5T} a(\tau)d\tau \tag{4}$$

The period T has to be sufficiently long so that the fluctuations in equation (4) are averaged to zero (Figure 2),

$$\bar{a}'(t) = \frac{1}{T}\int_{t-0.5T}^{t+0.5T} a'(\tau)d\tau = 0 \tag{5}$$

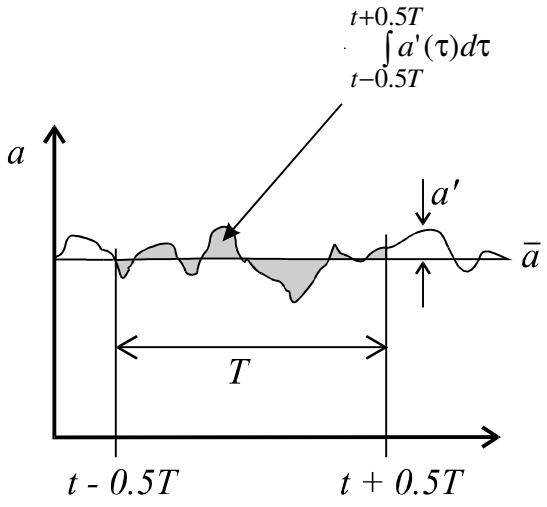

Figure 2.

In other words, T must be of sufficiently long duration so that dividing $\int_{t-0.5T}^{t+0.5T} a'(\tau)d\tau$ by T yields a result that is very close to zero. Furthermore, it will be assumed that the time period T is not so long that measurable changes in the average values (such as $\bar{a}$) would occur. Therefore, during the period T, the average value $\bar{a}$ of the instantaneous quantity a can be viewed as constant. Using equations (4) and (5) and accepting these stipulations, it is straightforward to show

$$\overline{a+b} = \overline{\bar{a}+a'+\bar{b}+b'} = \bar{\bar{a}} + \bar{a'} + \bar{\bar{b}} + \bar{b'} = \bar{a} + \bar{b} \tag{6}$$

In equation (6), a and b are two fluctuating quantities. The time-averages of the fluctuations a' and b' were set to zero, in accordance with (5). Similarly, if c is a constant then

$$\overline{ca} = \overline{c(\bar{a}+a')} = \overline{c\bar{a}} + \overline{ca'} = c\bar{a} \qquad (c \text{ is a constant}) \tag{7}$$

Another helpful formula is

$$\overline{ab} = \overline{(\bar{a}+a')(\bar{b}+b')} = \overline{\bar{a}\bar{b}+a'\bar{b}+\bar{a}b'+a'b'} = \overline{\bar{a}\bar{b}}+\overline{a'\bar{b}}+\overline{\bar{a}b'}+\overline{a'b'} = \bar{a}\bar{b}+0+0+\overline{a'b'}$$
$$\overline{ab} = \bar{a}\bar{b}+\overline{a'b'} \tag{8}$$

Note that the time-average of the *product* of the two fluctuations a' and b' cannot be set to zero; for instance, if $b = a$, the product of the two fluctuations would be $\overline{a'a'} = \overline{a'^2}$. Clearly, a squared term like a'^2 will always be positive, and so its time-average will not be zero. On the other hand, terms like $\overline{a'\bar{b}}$ can be regarded as the average of a fluctuation a' multiplied by a *constant* value $\bar{b}$. Therefore, just as in the case of the term $\overline{ca'}$ in equation (7), the term $\overline{a'\bar{b}}$ is zero.

Since the order of integration over τ and of differentiation with respect to a coordinate x_i commute,

$$\overline{\frac{\partial a}{\partial x_i}} \equiv \frac{1}{T}\int_{t-0.5T}^{t+0.5T}\frac{\partial a}{\partial x_i}(\tau)\mathrm{d}\tau = \frac{\partial}{\partial x_i}\frac{1}{T}\int_{t-0.5T}^{t+0.5T}a(\tau)\mathrm{d}\tau \tag{9}$$

Equation (9) can thus be simply rewritten,

$$\overline{\frac{\partial a}{\partial x_i}} = \frac{\partial \bar{a}}{\partial x_i} \tag{10a}$$

Equation (10a) implies that the ∇ operator, which takes derivatives with respect to position, also commutes with time-averaging:

$$\overline{\nabla a} = \nabla \bar{a} \tag{10b}$$

Similarly, it can be proven that

$$\overline{\frac{\partial a}{\partial t}} = \frac{\partial \bar{a}}{\partial t} \tag{10c}$$

Equations (5) to (10) will be of assistance in time-averaging the differential conservation equations.

i) Time-Averaged Equation of Continuity (differential mass balance). The differential equation of continuity is

$$\frac{\partial \rho}{\partial t} + \nabla \cdot \rho\, \mathbf{v} = 0 \tag{11}$$

Substituting $\rho = \bar{\rho} + \rho'$, $\mathbf{v} = \bar{\mathbf{v}} + \mathbf{v}'$, and time-averaging:

$$\overline{\frac{\partial(\bar{\rho}+\rho')}{\partial t} + \nabla \cdot (\bar{\rho}+\rho')(\bar{\mathbf{v}}+\mathbf{v}') = 0} \quad \rightarrow \quad \frac{\partial(\bar{\rho}+\bar{\rho}')}{\partial t} + \nabla \cdot (\overline{\bar{\rho}\bar{\mathbf{v}}} + \overline{\rho'\bar{\mathbf{v}}} + \overline{\mathbf{v}'\bar{\rho}} + \overline{\rho'\mathbf{v}'}) = 0 \tag{12}$$

Simplifying,

$$\frac{\partial \bar{\rho}}{\partial t} + \nabla \cdot (\bar{\rho}\bar{\mathbf{v}} + \overline{\rho' \mathbf{v}'}) = 0 \tag{13}$$

For an incompressible fluid, $\bar{\rho}$ is a constant and ρ' is zero; therefore, the differential mass balance (13) becomes

$$\nabla \bullet \bar{\mathbf{v}} = 0 \qquad \text{(incompressible fluid)} \tag{14}$$

ii). Time-Averaged Equation of Motion (differential momentum balance). The fluid is assumed to be Newtonian, incompressible, and of constant viscosity. The differential equation of motion is then given by (note that the convective term $\mathbf{v} \bullet \nabla \mathbf{v}$ can only be directly expanded in Cartesian coordinates)

$$\rho\left(\frac{\partial \mathbf{v}}{\partial t} + \mathbf{v} \cdot \nabla \mathbf{v}\right) = \mathbf{B} - \nabla p + \mu \nabla^2 \mathbf{v} \tag{15}$$

The body force is assumed to be gravitational only, and thus equal to $-\rho\mathbf{g}$ which does not fluctuate for an incompressible fluid. Substituting $\mathbf{v} = \bar{\mathbf{v}} + \mathbf{v}'$ and $p = \bar{p} + p'$, followed by time-averaging yields

$$\overline{\rho\left(\frac{\partial(\bar{\mathbf{v}} + \mathbf{v}')}{\partial t} + (\bar{\mathbf{v}} + \mathbf{v}') \cdot \nabla(\bar{\mathbf{v}} + \mathbf{v}')\right)} = \mathbf{B} - \overline{\nabla(\bar{p} + p')} + \overline{\mu \nabla^2 (\bar{\mathbf{v}} + \mathbf{v}')} \tag{16}$$

which simplifies to

$$\rho\left(\frac{\partial \bar{\mathbf{v}}}{\partial t} + \bar{\mathbf{v}} \cdot \nabla \bar{\mathbf{v}} + \overline{\mathbf{v}' \cdot \nabla \mathbf{v}'}\right) = \mathbf{B} - \nabla \bar{p} + \mu \nabla^2 \bar{\mathbf{v}} \tag{17}$$

From the continuity equation for incompressible flow,

$$\nabla \bullet \mathbf{v} = 0$$

what implies

$$\nabla \bullet (\bar{\mathbf{v}} + \mathbf{v}') = \nabla \bullet \bar{\mathbf{v}} + \nabla \bullet \mathbf{v}' = 0 \tag{18}$$

From equation (14) above, for incompressible turbulent flow $\nabla \bullet \bar{\mathbf{v}} = 0$. When substituted into equation (18) this implies

$$\nabla \bullet \mathbf{v}' = 0 \tag{19}$$

Since $\nabla \bullet \mathbf{v}'$ equals zero, adding $\overline{\mathbf{v}'(\nabla \cdot \mathbf{v}')}$ to $\overline{\mathbf{v}' \cdot \nabla \mathbf{v}'}$ on the left of equation (17) will not alter the equation. Furthermore, these two terms can be combined using the vector identity $\mathbf{v}'(\nabla \bullet \mathbf{v}') + \mathbf{v}' \bullet \nabla \mathbf{v}' = \nabla \bullet \mathbf{v}'\mathbf{v}'$, so that $\overline{\mathbf{v}'(\nabla \cdot \mathbf{v}')} + \overline{\mathbf{v}' \cdot \nabla \mathbf{v}'} = \overline{\nabla \cdot \mathbf{v}'\mathbf{v}'}$. With these modifications, equation (17) becomes

$$\rho\left(\frac{\partial \bar{\mathbf{v}}}{\partial t} + \bar{\mathbf{v}} \cdot \nabla \bar{\mathbf{v}} + \overline{\nabla \cdot \mathbf{v}'\mathbf{v}'}\right) = \mathbf{B} - \nabla \bar{p} + \mu \nabla^2 \bar{\mathbf{v}} \tag{20}$$

Most often, the term $\overline{\nabla \cdot \mathbf{v}'\mathbf{v}'}$ is written on the right hand side, with the density ρ (a constant by assumption) inside the divergence,

$$\rho\left(\frac{\partial \bar{\mathbf{v}}}{\partial t} + \bar{\mathbf{v}} \cdot \nabla \bar{\mathbf{v}}\right) = \mathbf{B} - \nabla \bar{p} + \mu \nabla^2 \bar{\mathbf{v}} - \overline{\nabla \cdot \rho \mathbf{v}'\mathbf{v}'} \tag{21}$$

Equation (21) is the time-averaged differential momentum balance for an incompressible, constant viscosity Newtonian fluid. The quantity $-\rho\mathbf{v}'\mathbf{v}'$ in the last term of equation (21) is often referred to as the "**Reynolds stress**." The *i,j*th Reynolds stress is

$$(-\overline{\rho \mathbf{v}'\mathbf{v}'})_{ij} = -\overline{\rho v'_i v'_j} \tag{22}$$

Equation (21) is straightforward to expand in Cartesian coordinates. The easiest way to expand it in curvilinear coordinates is by adding the Reynolds stresses, $-\overline{\nabla \cdot \rho \mathbf{v}'\mathbf{v}'}$, to the corresponding curvilinear momentum balance equation after replacing all velocities and pressures by their respective time-averaged values. An example will be encountered later during the discussion of pipe flow when equation (21) will be expanded in cylindrical coordinates. When in doubt, one can always time-average the expanded curvilinear expressions directly. Also, if fluctuations in density or viscosity were allowed, then additional terms would have appeared in equation (21). Should it be necessary to account for such effects, the appropriate modifications can be derived following a procedure analogous to that used above.

Physically, equation (21) states that the change in the average velocity that a fluid element moving *at the average velocity* would experience is equal to the sum of the time-averaged body, pressure, and viscous forces acting on the element, plus a contribution due to the Reynolds stresses. The negative divergence of the Reynolds stresses represents *convective* momentum transfer due to the random motion of macroscopic fluid packets (eddies). Figure 3 illustrates momentum transfer due to this random motion. For instance, if a fluid packet is transferred by a turbulent fluctuation from position y_2 to y_1 as illustrated in the figure, then the momentum in the x direction at y_1 will be increased since the incoming fluid packet has a greater x-momentum than the fluid being displaced. It is this turbulent motion of the fluid packets that makes for a more effective momentum (as well as mass and energy) transport than in laminar flow.

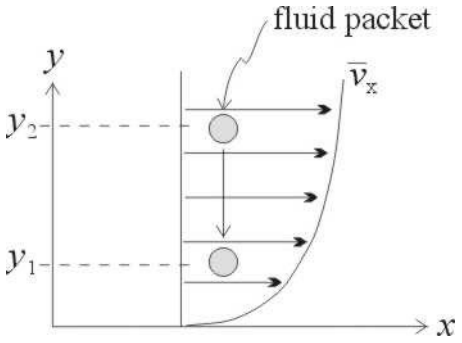

Figure 3

Using analogous procedures, one could also develop equations for a time-averaged differential energy balance. The remainder of the handout will focus on understanding turbulence as it manifests in momentum transport.

The Stress Tensor in Turbulent Flow. The stress tensor for a Newtonian fluid is given by

$$\sigma_{ij} = -p\delta_{ij} - (2/3)\,\mu\left(\frac{\partial v_k}{\partial x_k}\right)\delta_{ij} + \mu\left(\frac{\partial v_i}{\partial x_j} + \frac{\partial v_j}{\partial x_i}\right) \tag{23}$$

It will be assumed that the fluid is incompressible ($\partial v_k/\partial x_k = 0$) and of constant viscosity. Substituting $p = \bar{p} + p'$, $\mathbf{v} = \bar{\mathbf{v}} + \mathbf{v}'$, and time averaging,

$$\overline{\sigma_{ij}} = -\bar{p}\,\delta_{ij} + \mu\left(\frac{\partial \overline{v_i}}{\partial x_j} + \frac{\partial \overline{v_j}}{\partial x_i}\right) \tag{24}$$

Using similar manipulations as in handout #8 where the differential momentum balance was derived for a Newtonian fluid, we could show that the first term in equation (24) gives rise to the $-\nabla\bar{p}$ in the time-averaged momentum balance (equation (21)) while the second term gives rise to $\mu\nabla^2\bar{\mathbf{v}}$. As discussed earlier, this second, viscous stress term $\mu\left(\frac{\partial \overline{v_i}}{\partial x_j} + \frac{\partial \overline{v_j}}{\partial x_i}\right)$ is often said to cause momentum transport by "conduction." Conduction of momentum results from molecular level processes such as the interchange of fluid molecules between parts of fluid moving at different speeds, or from the forces generated by fluid molecules "rubbing" against each another. Because conductive momentum transport also occurs in laminar flow; it is customary to think of the viscous term $\mu\nabla^2\bar{\mathbf{v}}$ in equation (21) as laminar in nature. In contrast, the Reynolds stresses represent momentum transport due to the turbulent *convection* of macroscopic packets of fluid (eddies) as illustrated in Figure 3. The *i,j*th Reynolds stress can be designated by the notation $\overline{\sigma^T_{ij}}$

$$\overline{\sigma^T_{ij}} = -\overline{\rho v'_i v'_j} \tag{25}$$

and added to the Newtonian fluid stress (equation (24)) to produce the "**total stress**" $\overline{\sigma_{ijTOT}}$

$$\overline{\sigma_{ijTOT}} = \overline{\sigma_{ij}} + \overline{\sigma^{T}{}_{ij}} = -\overline{p}\,\delta_{ij} + \mu\left(\frac{\partial \overline{v_i}}{\partial x_j} + \frac{\partial \overline{v_j}}{\partial x_i}\right) - \overline{\rho v'_i\, v'_j} \tag{26}$$

The total stress includes not only viscous and pressure stresses, but also the *convection* term $-\overline{\rho v'_i\, v'_j}$. The total stress is symmetric. In terms of the total stress, the time-averaged differential momentum balance (equation (21)) is written

$$\rho\left(\frac{\partial \overline{\mathbf{v}}}{\partial t} + \overline{\mathbf{v}} \cdot \nabla \overline{\mathbf{v}}\right) = \mathbf{B} + \nabla \cdot \overline{\boldsymbol{\sigma}_{ijTOT}} \tag{27}$$

For example, for flow in two dimensions that can be fully described by a time-averaged velocity $\overline{v}_1(x_2)$, equation (26) predicts an effective total shear stress $\overline{\sigma_{21TOT}}$

$$\overline{\sigma_{21TOT}} = \mu \frac{\partial \overline{v_1}}{\partial x_2} - \overline{\rho v'_1\, v'_2} \tag{28}$$

Equation (28) can be rewritten in terms of the **eddy viscosity** ε

$$\varepsilon = -\left(\overline{v'_1\, v'_2}\right) / \left(\frac{\partial \overline{v_1}}{\partial x_2}\right) \tag{29}$$

to appear as

$$\overline{\sigma_{21TOT}} = (\mu + \rho\varepsilon) \frac{\partial \overline{v_1}}{\partial x_2}$$

A single eddy viscosity can be defined for any flow characterized by a single time-averaged velocity component that depends on a single coordinate variable. The purpose of the eddy viscosity is simply to rewrite equation (28) into a form similar to that for laminar flow. Next to a solid wall where the fluctuations in velocities, and thus the Reynolds stresses, must approach zero, the eddy viscosity will also approach zero. Therefore, in general, the eddy viscosity *varies* with position.

If mathematical expressions were available for the Reynolds stresses, then they could be inserted into the equation for the stress tensor or the momentum balance. To avoid the introduction of new unknowns, such expressions should be written in terms of unknowns already present in the equations (such as derivatives of the average velocities). Indeed, several such semiempirical expressions for the Reynolds stresses are available. These expressions can be especially useful for modeling simple flows such as when a single time-average velocity component $\overline{v_1}$ varies with the distance x_2 from a solid wall. We will consider two such relations for the Reynolds stresses.

i). Prandtl's Mixing Length. Prandtl imagined that the eddies in turbulent flow move around similar to the manner in which molecules move about in a gas. By drawing an analogy to viscosity expressions for gases from kinetic theory, he suggested that

$$\overline{\sigma^{T}{}_{21}} = -\overline{\rho v'_1\, v'_2} = \rho L^2 \left|d\overline{v_1}/dx_2\right| d\overline{v_1}/dx_2 \tag{30}$$

where L is called the "**mixing length**." Usually, L is set to equal $L = k_1 x_2$ where k_1 is a constant and x_2 is the distance from a solid wall. Experimentally, $k_1 = 0.36$ has been shown to work reasonably well. As required, the Prandtl Mixing Length expression reduces to zero at the solid wall. The analogy of momentum transfer by turbulence to that by molecules in a gas is rather poor, but expression (30) has nevertheless proven useful. Expression (30) is most accurate sufficiently far from the solid wall (i.e. in the **turbulent core** regime discussed later).

ii). Deissler's Formula for the Region Near the Wall. Based on experimental results, Deissler suggested that near the pipe wall (i.e. in the **laminar sublayer** and the **transition region** discussed later) a more accurate expression for the Reynolds stress $\overline{\sigma^T_{21}}$ than equation (30) is

$$\overline{\sigma^T_{21}} = -\overline{\rho v'_1 v'_2} = \rho n^2 \overline{v_1}\, x_2 \,(1 - \exp\{-\rho n^2 \overline{v_1}\, x_2/\mu\})\, d\overline{v_1}/dx_2 \qquad (31)$$

where the constant n has been experimentally estimated as $n = 0.124$. Again, the Reynolds stress reduces to zero at the wall.

Turbulent Flow Past Solid Surfaces.

i). Law of the Wall. Dimensional analysis can suggest which dimensionless groups affect the time-averaged velocity distribution near a solid wall. The dependent variable of interest is the velocity $\overline{v_1}$ parallel to the wall. The wall is assumed to be smooth and it is postulated that $\overline{v_1}$ will depend on the distance x_2 from the wall, the fluid density ρ, the fluid viscosity μ, and the wall shear stress σ_{21W} (i.e. $\overline{v_1} = f(x_2, \rho, \mu, \sigma_{21W})$) . σ_{21W} is a quantity local to the wall region that is sensitive to, and therefore accounts for, the rate of fluid flow past the wall. Since the near-wall region is being analyzed, it is desirable to use local quantities like σ_{21W} rather than quantities defined far from the wall (such as the maximum velocity).

Applying the Buckingham Pi Theorem, ρ, μ, and σ_{21W} are chosen as the repeating parameters (note: since x_2 varies even if all other parameters are fixed, it is more convenient to regard it as an independent variable than as a parameter). From the dimensional analysis, two dimensionless groups emerge

$$\overline{v_1}^* = \overline{v_1} / \sqrt{\sigma_{21w}/\rho} = \overline{v_1} / v_f \qquad x_2^* = x_2 \sqrt{\sigma_{21w}\,\rho}/\mu \qquad (32)$$

so that

$$\overline{v_1}^* = f(x_2^*) \qquad (33)$$

The "**frictional velocity**" $v_f = \sqrt{\sigma_{21w}/\rho}$ has been introduced in equation (32). Equation (33) suggests that $\overline{v_1}^*$ depends only on x_2^*, an observation that is sometimes referred to as the "**Law of the Wall**." Below, experimental evidence will be considered to see how well this law holds in practice.

ii). Isotropic versus Wall Turbulence. Far from any walls, turbulence can be isotropic in the sense that turbulent quantities become independent of direction. For instance, in isotropic turbulent flow, the mean squared velocity fluctuation $\overline{v_1'^2}$ in the x_1 direction would be equal to the mean squared velocity fluctuations $\overline{v_2'^2}$ and $\overline{v_3'^2}$. On the other hand, near a solid surface the velocity fluctuations along different directions are influenced differently by the presence of the surface, and the turbulence becomes *anisotropic*. Such anisotropic turbulence is sometimes referred to as wall turbulence. Since typical flows of interest to chemical engineering involve contact with solid surfaces, anisotropic turbulence is of significant practical interest. Below, an example of experimental measurements of turbulence anisotropy in pipe flow will be presented.

iii). Internal Turbulent Flow (Pipe Flow). Experiments indicate that the Law of the Wall holds quite well for pipe flow. The plot in Figure 4 shows data from pipe flow measurements for different systems. Indeed, the different experiments collapse onto a single curve when displayed as $\overline{v_z}^*$ vs. x_2^*. $\overline{v_z}^*$ is the time-averaged velocity in the z-direction (Figure 5), and the distance x_2 from the pipe wall is related to the radial distance r from the center of the pipe by

$$x_2 = R - r \tag{34}$$

R is the pipe radius. The curve in Figure 4 is the function f in the relation $\overline{v_z}^* = f(x_2^*)$ (equation (33)). By pure fortuitousness, the law of the wall persists remarkably far from the solid wall, despite being specifically derived for the near-wall region only. In fact, it is often assumed to hold with negligible error across the entire cross-section of a pipe, $0 < x_2^* < R\sqrt{\sigma_{21w}\,\rho}\,/\mu$.

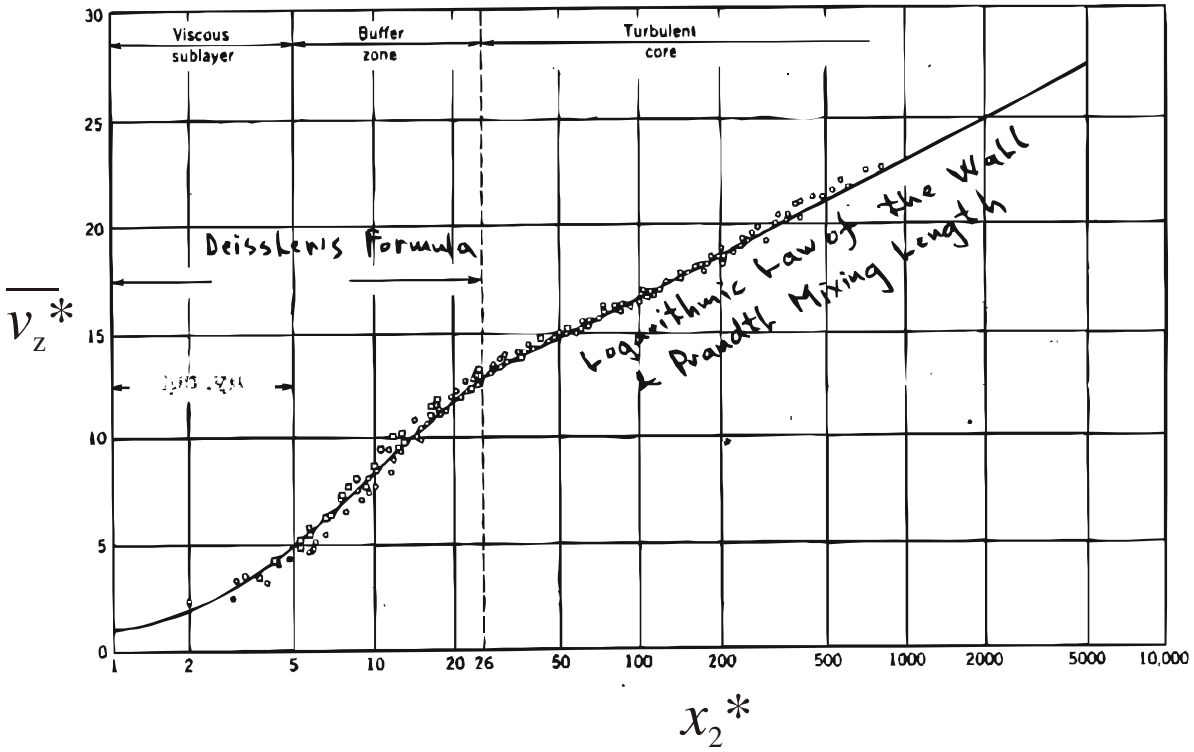

Figure 4

(Figure 4 is adapted from *Schaum's Outline of Theory and Problems of Fluid Dynamics*, W.F. Hughes, J.F. Brighton, McGraw-Hill, New York, 1991).

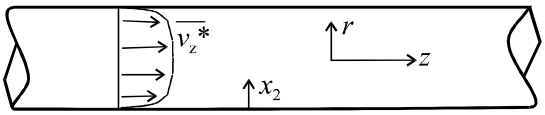

Figure 5

The region right next to the pipe wall, where $x_2^* < 5$, is referred to as the **laminar sublayer**. Here, turbulent fluctuations are strongly suppressed due to the requirement that all fluctuations be zero at the wall. Since turbulence is suppressed, viscous effects dominate and the flow can be regarded as laminar. Momentum transport in the laminar sublayer occurs by viscous conduction (i.e. through the action of viscous forces between different layers of the fluid). Accordingly, the laminar sublayer is also referred to as the ***viscous* sublayer**. Next to the laminar sublayer is the **transition region**, approximately located between $5 < x_2^* < 30$. In the transition region, conductive viscous and convective turbulent momentum transport are of comparable magnitude. The transition region is also known as the ***buffer zone***. For $x_2^* > 30$ the flow is part of the **turbulent core**. Here, momentum transport by convective turbulent effects dominates while conductive viscous transport of momentum is of minor importance. The turbulent core is also referred to as the *free turbulent* or *fully developed turbulent* flow. The division between the three regions is somewhat conceptual, and need not be taken too literally. The velocity profile in turbulent flow is flatter in the central part of the pipe (i.e. in the turbulent core) than in laminar flow (Figure 6) due to the extra equalization of velocities brought about by the turbulent "mixing" of the fluid.

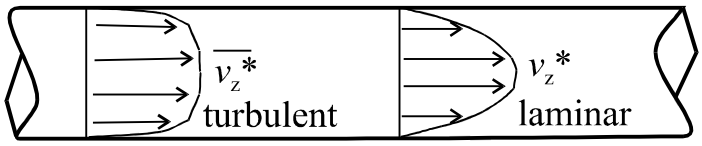

Figure 6.

As indicated in Figure 4, Deissler's formula for the Reynolds stress (equation (31)) holds for $x_2^* < 30$. This region includes the so-called transition layer ($5 < x_2^* < 30$) as well as the laminar sublayer ($x_2^* < 5$). The Prandtl mixing length expression (equation (30)) is most applicable to the turbulent core, $x_2^* > 30$. By inserting the Prandtl mixing length expression for the Reynolds stress $\overline{\sigma^T_{rz}}$ into the time-averaged momentum balance (equation (21)) and then solving for the velocity $\overline{v_z}$ * (x_2*), under certain approximations (i.e. viscous momentum transport negligible in the turbulent core, incompressible flow) it can be shown that in the turbulent core the time-averaged velocity varies as

$$\overline{v_z}^* = C_1 \ln(x_2^*) + C_2 \qquad \text{(turbulent core)} \qquad (35)$$

where C_1 and C_2 are constants. Experimental measurements indicate that a suitable choice for the values of these constants is $C_1 = 2.5$ and $C_2 = 5.5$. Equation (35) obeys the expected dimensionless form expressed by equation (33), and fits the data of Figure 4 in the turbulent core region. Equation

(35) is called at times the **Logarithmic Form of the Law of the Wall**. An alternate expression that is more convenient to use mathematically, but does not fit the data quite as well as equation (35) is

$$\overline{v_z}^* = 8.74\,(x_2^*)^{1/7} \qquad \text{(turbulent core)} \qquad (36)$$

The time-average velocity profile $\overline{v_z}^*$ in the laminar sublayer and the transition region could be analyzed using Deissler's formula (equation (31)) for the Reynolds stresses and the time-averaged momentum balance. In particular, this approach can be used to show that in the laminar sublayer ($x_2^* < 5$) the velocity profile obeys the simple relation $\overline{v_z}^* = x_2^*$.

Having outlined the behavior of the average velocity, we next consider the behavior of the fluctuation components of the velocities. Experimental measurements of the root-mean-square velocity fluctuations $\sqrt{\overline{v'^2_z}}$, $\sqrt{\overline{v'^2_r}}$, and $\sqrt{\overline{v'^2_\theta}}$ are plotted in Figure 7. The fluctuations are displayed as a function of the distance x_2/R from the pipe wall. The velocity fluctuations are normalized by the time-averaged maximum velocity $\overline{V}_{z\,\max}$ in the center of the pipe. From Figure 7, it is clear that maximum velocity fluctuations occur in the z-direction (i.e. the flow direction), while minimal fluctuations occur in the radial direction (i.e. perpendicular to the pipe walls). The turbulence is anisotropic at all radial positions, with the degree of anisotropy increasing closer to the pipe wall. Although not shown in Figure 7, very close to the pipe wall all of the velocity fluctuations rapidly drop to zero as the transition region and laminar sublayer are entered.

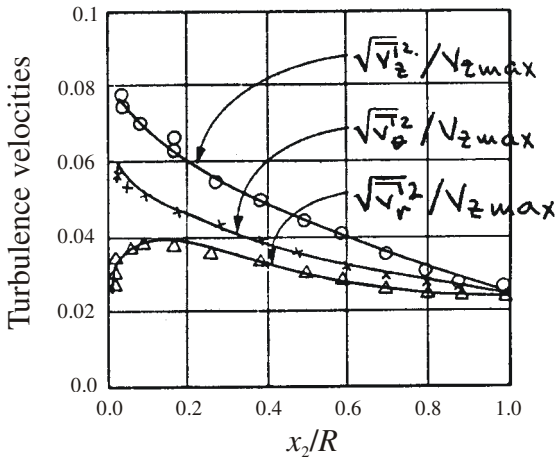

Figure 7. (Adapted from *Schaum's Outline of Theory and Problems of Fluid Dynamics*, W.F. Hughes, J.F. Brighton, McGraw-Hill, New York, 1991).

Figure 8 plots the Reynolds stress $-\rho\overline{v'_{x_2}\,v'_z}$ as a function of x_2/R. The Reynolds stress is normalized by the wall shear stress σ_{rzW}. From Figure 8 it is evident that the Reynolds stress is positive. The positive magnitude can be expected on physical grounds. For instance, consider that a velocity fluctuation in the positive radial direction occurs at a point in the flow. A velocity fluctuation in the positive radial direction corresponds to a *negative* velocity fluctuation v'_{x2} in the x_2 direction, $v'_{x2} < 0$. This is because the coordinate $x_2 = R - r$ points *opposite* to the radial coordinate r. As a result of the radial fluctuation, fluid will be brought to the point from a region that is closer to the center of the pipe. Since fluid toward the center of the pipe tends to flow faster in the z direction, the incoming fluid will

in general have a greater z-velocity than the fluid it displaces. Therefore, the incoming fluid will tend to produce a positive fluctuation $v'_Z > 0$. Accordingly, the product $v'_{x2}v'_Z$ of the radial and z-direction fluctuations tends to be negative, so that the Reynolds stress $-\overline{\rho v'_{x_2} v'_z}$ will have a positive value.

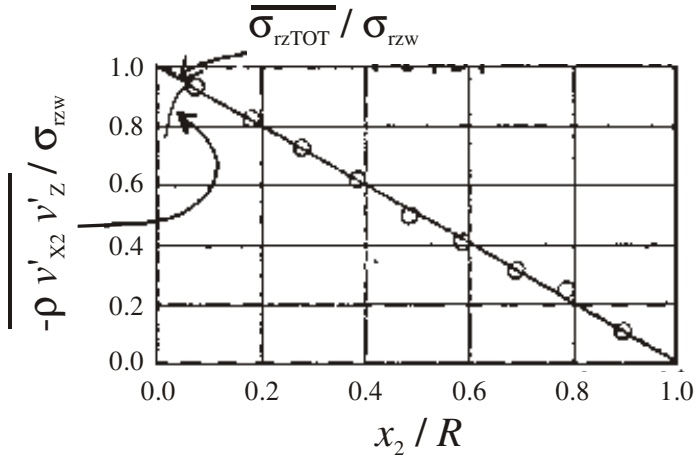

Figure 8. (Adapted from *Schaum's Outline of Theory and Problems of Fluid Dynamics*, W.F. Hughes, J.F. Brighton, McGraw-Hill, New York, 1991).

Further insight into the Reynolds stresses can be obtained by referring to the time-averaged equation of motion. For constant viscosity, incompressible turbulent flow in a pipe, the z-component of the time-averaged equation of motion (equation (21)) is

$$\rho\left(\frac{\partial \overline{v_z}}{\partial t} + \overline{v_r}\frac{\partial \overline{v_z}}{\partial r} + \frac{\overline{v_\theta}}{r}\frac{\partial \overline{v_z}}{\partial \theta} + \overline{v_z}\frac{\partial \overline{v_z}}{\partial z}\right) =$$
$$B_z - \frac{\partial \overline{p}}{\partial z} + \mu\left(\frac{\partial^2 \overline{v_z}}{\partial r^2} + \frac{1}{r}\frac{\partial \overline{v_z}}{\partial r} + \frac{1}{r^2}\frac{\partial^2 \overline{v_z}}{\partial \theta^2} + \frac{\partial^2 \overline{v_z}}{\partial z^2}\right) + \frac{1}{r}\frac{\partial r\overline{\sigma^T_{rz}}}{\partial r} + \frac{1}{r}\frac{\partial \overline{\sigma^T_{\theta z}}}{\partial \theta} + \frac{\partial \overline{\sigma^T_{zz}}}{\partial z} \qquad (37)$$

The last three terms in equation (37) involve the Reynolds stresses, where $\overline{\sigma^T_{rz}} = -\overline{\rho v'_r v'_z}$ is the r,z component of the Reynolds stress and so on. Equation (37) was obtained by writing out the cylindrical z-component momentum balance in terms of time-averaged quantities and then adding the Reynolds stress terms according to equation (21). Since the flow is fully developed, $\overline{v_z}$ and the Reynolds stresses do not vary with position z along the pipe. In addition, due to symmetry they also do not vary with θ. These considerations imply that $\overline{v_z}$ and the Reynolds stresses only depend on r. Furthermore, $\overline{v_r} = \overline{v_\theta} = 0$ and body forces are neglected. With these simplifications, equation (37) becomes

$$0 = -\frac{d\overline{p}}{dz} + \mu\left(\frac{d^2 \overline{v_z}}{dr^2} + \frac{1}{r}\frac{d\overline{v_z}}{dr}\right) + \frac{1}{r}\frac{dr\overline{\sigma^T_{rz}}}{dr} = -\frac{d\overline{p}}{dz} + \frac{1}{r}\frac{d}{dr}\left(r\mu\frac{d\overline{v_z}}{dr}\right) + \frac{1}{r}\frac{d}{dr}(r\overline{\sigma^T_{rz}})$$
$$0 = -\frac{d\overline{p}}{dz} + \frac{1}{r}\frac{d}{dr}\left(r\overline{\sigma_{rz}}\right) + \frac{1}{r}\frac{d}{dr}(r\overline{\sigma^T_{rz}}) = -\frac{d\overline{p}}{dz} + \frac{1}{r}\frac{d}{dr}\left(r\overline{\sigma_{rzTOT}}\right) \qquad (38)$$

Going from the first to the second line in equation (38), the term $\mu\,(\mathrm{d}\overline{v_z}/\mathrm{d}r)$ was recognized as the time-averaged viscous stress $\overline{\sigma_{rz}}$ for a Newtonian fluid. Then the viscous stress $\overline{\sigma_{rz}}$ and the Reynolds stress $\overline{\sigma_{rz}^{T}}$ were combined into the "total stress" $\overline{\sigma_{rz\mathrm{TOT}}}$ defined previously by equation (26), $\overline{\sigma_{\mathrm{ijTOT}}} = \overline{\sigma_{\mathrm{ij}}} + \overline{\sigma^{\mathrm{T}}{}_{\mathrm{ij}}}$. Integrating equation (38) and applying the "center of flow" symmetry boundary condition, $\overline{\sigma_{rz\mathrm{TOT}}} = 0$ at $r = 0$, yields

$$\begin{aligned}\overline{\sigma_{rz\mathrm{TOT}}} &= (r/2)\,(\mathrm{d}\overline{p}/\mathrm{d}z) = (1 - x_2/R)\,(R/2)(\mathrm{d}\overline{p}/\mathrm{d}z)\\ &= (R/2)(\mathrm{d}\overline{p}/\mathrm{d}z) - x_2/R\,(R/2)(\mathrm{d}\overline{p}/\mathrm{d}z)\end{aligned} \qquad (39)$$

Equation (39) states that the total shear stress $\overline{\sigma_{rz\mathrm{TOT}}}$ decreases *linearly* as x_2/R increases, with a slope given by $-(R/2)(\mathrm{d}\overline{p}/\mathrm{d}z)$. In the turbulent core, $\overline{\sigma_{rz\mathrm{TOT}}} \approx \overline{\sigma_{rz}^{T}}$ to a very good approximation since turbulent shear stresses dominate viscous shear stresses. Therefore, across the turbulent core, it is expected that the turbulent shear stress will vary linearly with x_2/R. This is indeed borne out by the data in Figure 8. Also plotted in Figure 8 is the total shear stress, given by a straight line decreasing from 1 at $x_2/R = 0$ to 0 at $x_2/R = 1$. It is clear that the approximation $\overline{\sigma_{rz\mathrm{TOT}}} \approx \overline{\sigma_{rz}^{T}}$ holds across most of the pipe, since the curves for $\overline{\sigma_{rz\mathrm{TOT}}}$ and $\overline{\sigma_{rz}^{T}}$ are coincident above $x_2/R > \sim 0.1$ (for this particular set of measurements). For $x_2/R < \sim 0.1$ the flow passes from the turbulent to the transition and laminar sublayer regimes, and the Reynolds stress decreases due to its suppression by the vicinity of the solid wall.

iv). External Turbulent Flow Over a Flat Plate. As discussed previously, external flow over a solid surface can be conceptualized as consisting of a potential flow and a boundary layer region. The potential flow region is laminar. The boundary layer will start as laminar at the upstream edge of the solid surface or body, but will turn turbulent once it exceeds a certain thickness. The position at which the laminar to turbulent transition occurs is denoted by $x_1 = x_{1\mathrm{tr}}$ as illustrated in Figure 9. If the length L of the plate is too short, so that $L < x_{1\mathrm{tr}}$, then the transition will not be reached.

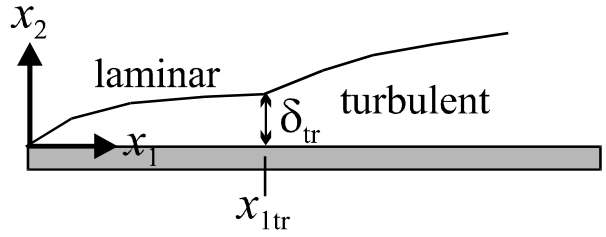

Figure 9

Measurements on turbulent boundary layers on flat plates indicate that the Law of the Wall (equation (33)) holds very well, with experimental results looking very similar to those for pipe flow shown in Figure 4. In addition, the laminar sublayer, the transition region, and turbulent flow occupy similar distances from the plate as they did in the case of pipe flow: $x_2^* < 5$ for laminar sublayer, $5 < x_2^* < 30$

for the transition region, and $30 < x_2^* < \delta^*$ for the turbulent region. Here $\delta^* = \delta \sqrt{\sigma_{21w} \rho} / \mu$ is the value of x_2^* at the outer periphery of the boundary layer. For $x_2^* > \delta^*$, the flow becomes laminar again as the potential flow region is entered. Note that x_2^* is as defined previously in equation (32), $x_2^* = x_2 \sqrt{\sigma_{21w} \rho} / \mu$. Except at the outermost part of the boundary layer where the potential flow region is approached, the mean velocity in the turbulent region obeys the logarithmic form of the Law of the Wall given previously in equation (35),

$$\overline{v_1}^* = 2.5 \ln(x_2^*) + 5.5 \tag{40}$$

Alternately, the power law expression (36) can also be used to represent the velocity profile in the turbulent part of the boundary layer,

$$\overline{v_1}^* = 8.74 (x_2^*)^{1/7} \tag{41}$$

Furthermore, in the turbulent part of the boundary layer similar anisotropy is observed for the time-averaged fluctuations $\sqrt{\overline{v'^2_1}}$, $\sqrt{\overline{v'^2_2}}$, and $\sqrt{\overline{v'^2_3}}$ as for the case of pipe flow (Figure 7). However, in contrast to pipe flow, due to the difference in flow geometry the total shear stress in the boundary layer does not decrease linearly with distance from the plate; rather, it decreases in a slightly sigmoidal fashion.

Equation (41) is convenient for evaluation of the shear stress on the plate, σ_{21P}, as well as the variation of the turbulent boundary layer thickness δ with position along the plate. Using the definitions of $\overline{v_1}^*$ and x_2^* from equation (32), equation (41) becomes

$$\overline{v_1} / \sqrt{\sigma_{21P} / \rho} = 8.74 (x_2 \sqrt{\sigma_{21P} \rho} / \mu)^{1/7} \tag{42}$$

At the outer edge of the boundary layer, $\overline{v_1} = V_o$ and $x_2 = \delta$ so that

$$V_o / \sqrt{\sigma_{21P} / \rho} = 8.74 (\delta \sqrt{\sigma_{21P} \rho} / \mu)^{1/7} \tag{43}$$

Rearranging equation (43) to isolate σ_{21P} produces

$$\sigma_{21P} = 0.0225 \rho V_o^2 (\mu / \rho V_o \delta)^{1/4} \tag{44}$$

Division of equation (42) by (43) gives

$$\overline{v_1} / V_o = (x_2 / \delta)^{1/7} \tag{45}$$

In handout 11, an integral momentum balance was applied to a control volume in the boundary layer to show that

$$\sigma_{21P} = \frac{d}{dx_1}\left[\int_0^{\delta} \rho\left(V_o - v_1\right)v_1 \mathrm{d}x_2\right] \tag{46}$$

Time-averaging equation (46) replaces the instantaneous velocity component v_1 with the time-average value $\overline{v_1}$,

$$\sigma_{21P} = \frac{\mathrm{d}}{\mathrm{d}x_1}\left[\int_0^{\delta} \rho\left(V_o - \overline{v_1}\right)\overline{v_1}\ \mathrm{d}x_2\right] \tag{46}$$

Note that a term - $\rho\overline{v_1'^2}$ was omitted in the integral of equation (46). There is no rigorous justification for this omission - at this stage it is simply done to simplify the subsequent mathematics. The ultimate test of the results derived based on equation (46) will have to be by comparison to experiment. Substituting equation (44) for σ_{21P} on the left hand side of equation (46), equation (45) for $\overline{v_1}$ on the right hand side of equation (46), and dividing the result by ρV_o^2 yields

$$0.0225\ (\mu / \rho V_o \delta)^{1/4} = \frac{\mathrm{d}}{\mathrm{d}x_1}\left[\int_0^{\delta} \left(1 - \left(\frac{x_2}{\delta}\right)^{1/7}\right)\left(\frac{x_2}{\delta}\right)^{1/7}\ \mathrm{d}x_2\right] \tag{47}$$

Integrating equation (47) and simplifying

$$0.231(\mu / \rho V_o)^{1/4} = \delta^{1/4}\ \mathrm{d}\delta/\mathrm{d}x_1$$

$$0.231(\mu / \rho V_o)^{1/4}\ \mathrm{d}x_1 = \delta^{1/4}\ \mathrm{d}\delta \tag{48}$$

Integrating equation (48) from the transition point $x_1 = x_{1tr}$, where the boundary layer thickness is δ_{tr}, to an arbitrary downstream position x_1 where the thickness is δ gives

$$\int_{x_{1tr}}^{x_1} 0.231(\mu / \rho V_o)^{1/4}\ \mathrm{d}x_1 = \int_{\delta_{tr}}^{\delta} \delta^{1/4}\ \mathrm{d}\delta \tag{49}$$

$$\delta^{5/4} - \delta_{tr}^{\ 5/4} = 0.289(\mu / \rho V_o)^{1/4}(x_1 - x_{1tr}) \tag{50}$$

If the position x_1 is far along the plate, so that $x_1 >> x_{1tr}$ and $\delta^{5/4} >> \delta_{tr}^{\ 5/4}$, then equation (50) may be simplified to

$$\delta = 0.371\ x_1(\mu / \rho V_o\, x_1)^{1/5} = 0.371\ x_1\,(Re_{x1})^{-1/5} \tag{51}$$

In equation (51), $Re_{x1} = \rho V_o\, x_1 / \mu$. Inserting equation (51) into equation (44) produces an expression for σ_{21P}

$$\sigma_{21P} = 0.0288 \rho V_o^2 \, (Re_{x1})^{-1/5} \tag{52}$$

The total drag force F_f on a flat plate of length L and width W, with boundary layers both on top and bottom of the plate, equals

$$F_f = 2 \int_0^W \int_0^L \sigma_{21p} dx_1 dx_3 \tag{53}$$

Inserting equation (52) into equation (53) and integrating,

$$F_f = 0.072 \rho V_o^2 WL (Re_L)^{-1/5} \tag{54}$$

The drag coefficient C_D is (recall: $C_D = F_f / (A \, \rho V_o^2/2)$ where the reference area A equals WL)

$$C_D = 0.144 (Re_L)^{-1/5} \tag{55}$$

Equations (51), (52), (54) and (55) all apply to turbulent boundary layers. Equation (51) shows that the thickness of a turbulent boundary layer increases as $x_1^{4/5}$, what is significantly faster than the $x_1^{1/2}$ increase observed for laminar boundary layers (see handout 11 for discussion of laminar boundary layers). The wall shear stress σ_{21P} (equation (52)) decreases with $x_1^{-1/5}$, to be compared to the faster decrease with $x_1^{-1/2}$ observed for laminar boundary layers. It should be kept in mind that equations (51) to (55) assume that $x_1 >> x_{1tr}$. Also, comparison to experiment shows that because of limits on the applicability of the velocity profile expression (41) on which all of the above derivations were based, the results derived should not be used if Re exceeds 10^7 or for plates whose surfaces are not smooth.

If the position x_{1tr} at which the boundary layer passes from laminar to turbulent is known, then greater accuracy may be achieved by applying laminar equations to the laminar portion of the boundary layer and turbulent equations to the turbulent part. For instance, the total shear drag on the plate could be calculated from

$$F_f = (\rho V_o^2/2) \, (C_{DL} A_L + C_{DT} A_T) \tag{56}$$

where C_{DL} is the drag coefficient for the laminar boundary layer and A_L is the area that the laminar boundary layer covers, and C_{DT} and A_T are the corresponding quantities for the turbulent boundary layer. However, it may be difficult to specify x_{1tr}. Usually, as long as $Re_L = \rho V_o L / \mu$ remains below 1×10^5 the entire boundary layer remains laminar. Under carefully controlled conditions when disturbances such as mechanical vibrations in the incoming stream are minimized, the entire boundary layer may remain laminar even up to Re_L of ~ 4×10^6. In any case, as the Reynolds number increases the onset of turbulence first appears at the downstream edge of the plate ($x_1 \approx L$) since this is where Re_{x1} has its largest value, $Re_{x1} = Re_L$. Additional increase in the Reynolds number would shift the laminar to turbulent transition closer to the leading edge of the plate.

v). Other Turbulent Flows. Turbulence can also occur when no solid surface or object is nearby. One example is a jet of fluid emerging into a quiescent reservoir. Another is the wake behind an object in external flow. Such "**free turbulence**" will not be discussed in detail here, except to state that many

types of turbulent flows continue to be experimentally and mathematically characterized. Specialized texts dealing with turbulent flows are available, e.g. P.S. Bernard and J.M. Wallace, *Turbulent Flow: Analysis, Measurement and Prediction*, Wiley, 2002.